Hindawi
Advances in Civil Engineering
Volume 2018, Article ID 2057940, 9 pages
https://doi.org/10.1155/2018/2057940

Research Article

Reinforcing Effect of Carbon Nanotubes/Surfactant Dispersions in Portland Cement Pastes

Oscar A. Mendoza Reales,[1] **Caterin Ocampo**,[2] **Yhan Paul Arias Jaramillo**,[2] **Juan Carlos Ochoa Botero**,[2] **Jorge Hernán Quintero**,[3] **Emílio C. C. M. Silva**,[4] **and Romildo Dias Toledo Filho**[1]

[1]*Universidade Federal do Rio de Janeiro, Rio de Janeiro, RJ, Brazil*
[2]*Universidad Nacional de Colombia, Medellín, Colombia*
[3]*Universidad de Medellín, Medellín, Colombia*
[4]*Petrobras Petróleo Brasileiro S.A., Rio de Janeiro, RJ, Brazil*

Correspondence should be addressed to Oscar A. Mendoza Reales; oscar@coc.ufrj.br

Received 13 March 2018; Accepted 16 May 2018; Published 11 June 2018

Academic Editor: Farhad Aslani

Copyright © 2018 Oscar A. Mendoza Reales et al. This is an open access article distributed under the Creative Commons Attribution License, which permits unrestricted use, distribution, and reproduction in any medium, provided the original work is properly cited.

Decoupling the individual effects of multiwalled carbon nanotubes (MWCNTs) and surfactants when used as reinforcement materials in cement-based composites is aimed in this study. Powder MWCNTs were dispersed in deionized water using different types of surfactants as chemical dispersing agents and an ultrasonic tip processor. Cement pastes with carbon nanotubes additions of 0.15% by mass of cement were produced in two steps: first, the MWCNT/surfactant dispersions were combined with the mixing water, and then, cement was added and mixed until a homogeneous paste was obtained. Mechanical properties of the pastes cured at 7 days were measured, and their fracture behavior was characterized using the linear elastic finite element analysis. It was found that the reinforcing effect of MWCNT was masked by the negative effect of surfactants in the cement matrix; nevertheless, nanotubes were capable of increasing both stress and strain capacity of the composite by controlling the crack propagation process at the tip of the crack.

1. Introduction

The mechanism by which multiwalled carbon nanotubes (MWCNTs) are able to enhance the mechanical properties of a cement matrix is called "bridge effect." MWCNTs are capable of creating a network of bridges that transmit load across cracks and pores [1], enhancing the load distribution within the matrix. This depends heavily on the length and aspect ratio of nanotubes [2]. Finite element modeling of beams under flexural stress has proposed that MWCNTs control crack propagation, allowing additional strain of the matrix by generating a sequential pullout of nanotubes while the crack develops, until complete pullout of the nanotubes is reached [3].

To guarantee adequate crack propagation control, MWCNTs must be well dispersed in the cement matrix [4], bridging the correct phases. This means that if MWCNTs agglomerate around individual hydrates instead of bridging neighboring ones, they will not have any effect on the stress distribution within the composite [5]. This is why the use of chemical dispersing agents, such as surfactants, is of prime importance to produce MWCNT-reinforced cement-based composites. Nevertheless, it is known that surfactants are able to interact with cement grains, modifying their hydration reaction [6, 7].

It is not clear that what is the extent of the reinforcing efficiency of MWCNT, but it has been found that small amounts of nanotubes increase the flexural strength of

cement-based matrices [8], identifying a correlation between their aspect ratio and reinforcing efficiency [9–11]. Additional parameters such as modulus of rupture [12], fracture energy, and fracture toughness [13] have also been identified to increase with the presence of MWCNT in the matrix.

On the contrary, some literature reports have shown decreases in mechanical properties of cement-based matrices. This behavior has been attributed to agglomeration phenomena of MWCNT when used in high volumes [14], to the presence of functional groups on the surface of the nanotubes able to interact chemically with the hydration reaction [12], or even to the presence of fine aggregates in the matrix for the case of mortars [15]. These conflicting reports are still a matter open for discussion [16], and the issue is a subject of several experimental and numerical studies [17–23]. This work aims at quantifying the reinforcing efficiency of MWCNT/surfactant dispersions, separating the effects induced by surfactants in the mechanical properties of the matrix from those induced by MWCNT.

2. Materials and Methods

The materials used were class G high sulfate-resistance (HSR) cement, industrial-grade pristine multiwalled carbon nanotubes (MWCNTs), sodium dodecyl sulfate (SDS), cetylpyridinium chloride (CPC), Triton X-100 (TX-100), and a viscosity modifying agent (VMA). Characterization of cement and VMA was performed by X-ray diffraction (XRD) and X-ray fluorescence (XRF). XRD tests were carried out in a diffractometer equipped with a Cu radiation source ($K\alpha$, $\lambda = 1{,}5418$ Å), from 4 to 70° 2θ with a step size of 0.05 and an accumulation time of 30 seconds. The XRF test was carried out using an X-ray fluorescence spectrometer capable of identifying elements from Na to U. Morphological characterization of the MWCNT was carried out using scanning transmission electron microscope (STEM) in the transmission mode with 20 kV acceleration and 225,000x magnification. MWCNTs were dispersed in deionized water using an ultrasonic bath; 1 ml of this dispersion was dropped in a #300 copper Formvar mesh and dried in a desiccator before imaging.

Deionized water was used to prepare MWCNT dispersions with 0.33% solid concentration of nanotubes using the three types of surfactants in 1 mM, 10 mM, and 100 mM concentrations. Surfactants were poured into the water and stirred for 5 minutes, and then solid MWCNTs were added to the mixture. An ultrasonic tip was used to apply a total energy of 390 J/g in a 500 W ultrasonic processor set to 40% amplitude in 20 seconds on/off cycles to avoid overheating the samples.

Three families of pastes were produced. A reference sample (Ref.) composed of cement and VMA at a water-to-cement ratio (w/c) of 0.55 and 1.0% VMA by mass of cement. The VMA was used as a stabilizing agent to guarantee that there is no static sedimentation of the pastes during curing. The second family, named plain (P), maintained the same w/c and VMA amount and was composed of water, surfactant, cement, and VMA; surfactant type and concentration were varied. The third family, named blended (B), maintained the same proportion as the P family, but 0.15% MWCNT by mass of cement was blended into them.

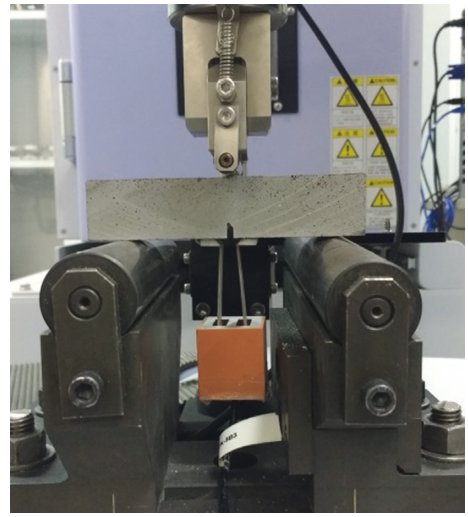

Figure 1: Experimental setup used to measure flexural strength by three-point bending.

Pastes were prepared by adding water, VMA, and the MWCNT/surfactant dispersions to the mixer. A 500 rpm rotation was maintained for 1 minute, cement was added, and rotation was increased to 2070 rpm during 1 minute and maintained constant for 5 minutes. Immediately after mixing, pastes were molded in $115 \times 115 \times 25$ mm slabs, vibrated for 60 seconds in a vibrating table, and cured in a high-humidity environment for 7 days.

At the testing stage, each slab was cut with a diamond saw to produce specimens for three-point bending. The obtained samples were $115 \times 25 \times 25$ mm beams with one 5 mm notch placed at midspan in one of the 25 mm faces. Two metal plates were glued at the edge of the notch to couple a clip gauge to measure crack mouth opening displacement (CMOD). The load application rate was varied to maintain a constant deformation rate at the CMOD of 0.03% of the initial gauge length per minute. Testing was carried out in a Shimadzu AGX 100 universal testing machine equipped with a 100 kN load cell. The experimental setup is presented in Figure 1. Flexural strength was calculated using the following equation:

$$\sigma = \frac{3PS}{2B\left(W - a_0\right)^2}, \tag{1}$$

where P is the applied load, S is the span (90 mm), B is the beam width (25 mm), W is the beam height (25 mm), and a_0 is the notch depth (5 mm).

Changes in the energy adsorption capacity (D) of the paste induced by the presence of MWCNTs were measured in the load versus deflection plots by adapting the procedure recommended by the RILEM technical committee 162 on test and design methods for steel fiber-reinforced concrete [24]. A typical load versus the deflection curve used for this procedure is presented in Figure 2. D was calculated as the area under the load-deflection curve after the maximum load, and it consists of two components: the contribution

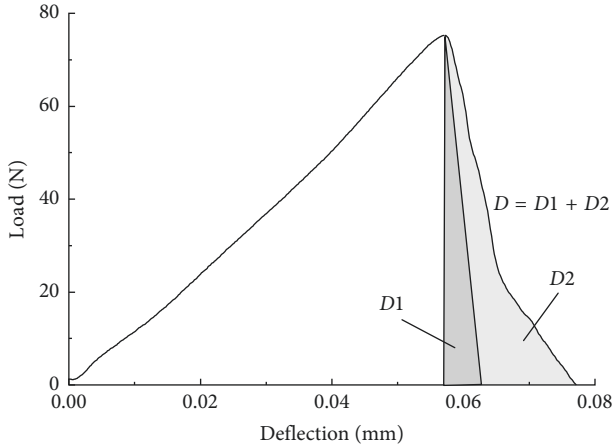

Figure 2: Typical load versus deflection curve used to calculate energy absorption capacity.

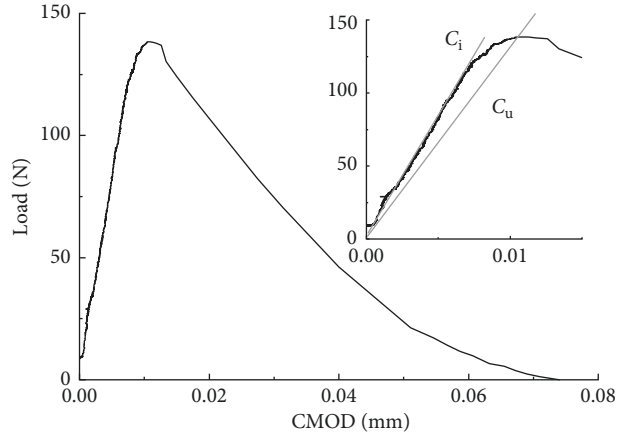

Figure 3: Typical load versus CMOD curve used to obtain C_i and C_u values.

from the cement paste ($D1$) and the contribution from the MWCNT ($D2$). $D1$ was approximated as a right triangle, and the slope of its hypotenuse was measured in pastes from the P family. This slope was then used to obtain $D2$ for the MWCNT-blended pastes (B family) by subtracting $D1$ from D.

Linear elastic fracture mechanics was used to characterize the influence of MWCNTs on the fracture behavior of the paste. This was achieved by employing a two-parameter facture model for concrete [25] to interpret the results of three-point bending tests on notched beams of the rectangular section. This model is based on the fact that the critical stress intensity factor (K_{Ic}) cannot be used to predict accurately the growth of a crack in quasibrittle materials such as concrete due to nonlinear slow crack growth before reaching the peak load [25]. The proposed model states that an effective crack extends before failure, which occurs only when the critical stress intensity factor K_I^S at the tip of the effective crack reaches a critical value K_{Ic}^S and, simultaneously, the crack tip opening displacement reaches its critical value ($CTOD_c$).

Compliance (C) was defined as $C = P/\text{CMOD}$. Two compliance parameters were used, initial compliance (C_i) and failure compliance (C_u), which correspond to the compliance at the initial crack length and at failure, respectively [26]. These parameters were obtained from experimental load versus CMOD plots from the slope of two linear fits as presented in Figure 3.

Linear elastic finite element simulations were used to obtain K_{Ic}^S, $CTOD_c$, and E values from the two-parameter model. The generic geometry used for the simulations is presented in Figure 4. The CMOD, CTOD, and K_I curves for the actual notch beam geometries were obtained as a function of the effective crack extension ($a_c - a_0$), as shown in Figure 5. An initial simulation was performed by applying $P = 100$ N and assuming $E = 10$ GPa. Young's modulus (E) of the material was calculated by matching the observed C_i. The $CMOD_c$ of the material was calculated by matching the observed C_u. The stress intensity factor was calculated using the energy release rate given by the J integral. The effective crack length a_c was determined by matching the observed CMOD at failure in the CMOD versus a_c curve. The critical values $CTOD_c$ and K_{Ic}^S were obtained directly from the simulation results at $a = a_c$.

3. Results and Discussion

This section presents the characterization of the raw materials used to produce cement pastes blended with MWCNT/surfactant dispersions; then, the individual effect of surfactants and MWCNT on the mechanical properties of the pastes is presented and discussed.

3.1. Materials Characterization. Chemical and mineralogical composition of cement and VMA was characterized using XRD and XRF. The obtained results are presented in Figure 6 and Table 1. Regarding the cement, the typical anhydrous phases were found, as well as anhydrite ($CaSO_4$) and gypsum ($CaSO_4{\cdot}2H_2O$) which were used as a setting time controller. Regarding the VMA, it was found that it is mainly composed of cellulose mixed with calcium and sodium chloride. An image of individual MWCNT is presented in Figure 7. Nanotubes were found to have a diameter of approximately 20 nm and typical length between 1 and 2 μm. For more details on the physical characteristic of the MWCNT, refer [27].

SDS was acquired in powder with a purity of 96% and a molecular weight of 288.38 g/mol. CPC was in powder form with 100% purity and a molecular weight of 358.0 g/mol. TX-100 was in liquid form with 98% purity and a molecular weight of 646.85 g/mol. These characteristics are according to the manufacturer.

3.2. Effect of Surfactants in the Density of Cement Paste. Apparent density was measured by water absorption for all the pastes from the B family after 7 days of curing; the obtained results are presented in Figure 8. It was found that density was dependent on the surfactant concentration used to disperse the MWCNT. A higher surfactant concentration led to a lower density, decreasing from 1.29 g/cm^3 for the

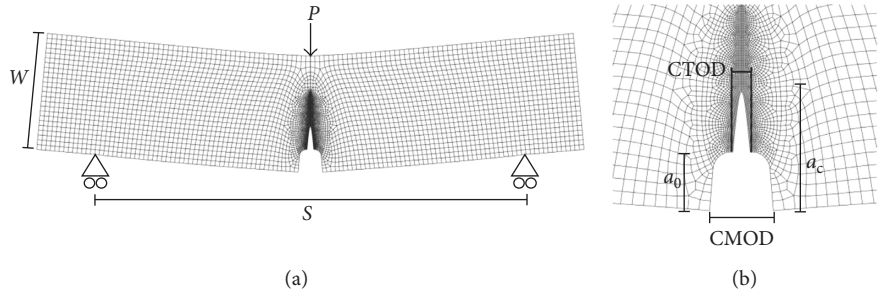

Figure 4: (a) General geometry and (b) detail of the notch and crack used in the finite element simulations (scale factor: 200).

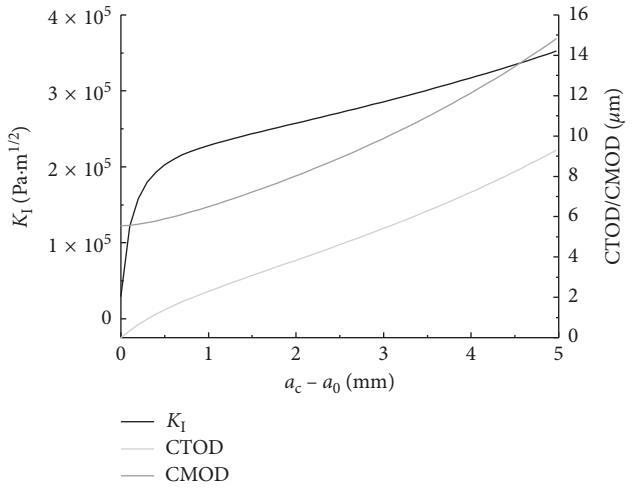

Figure 5: Typical K_I, CTOD, and CMOD versus effective crack extension plot.

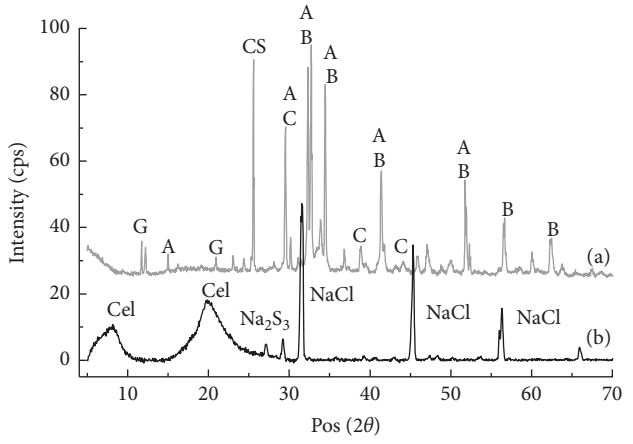

Figure 6: X-Ray diffraction pattern of (a) cement and (b) VMA (Cel: cellulose; G: gypsum ($CaSO_4{\cdot}2H_2O$); CS: anhydrite ($CaSO_4$); A; alite; (B) belite; C: calcite; cps: counts per second).

Table 1: XRF chemical composition of cement and VMA (LOI: loss on ignition).

	Cement	VMA
CaO	69.89	0.11
SiO_2	15.92	0.08
Fe_2O_3	5.33	—
Al_2O_3	3.94	0.01
SO_3	3.37	1.3
MgO	0.59	0.01
TiO_2	0.19	—
Na_2O	—	2.50
Cl	—	0.80
LOI	0.77	95.2

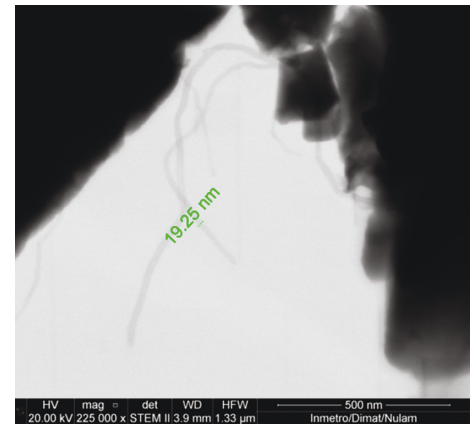

Figure 7: TEM image of MWCNT.

reference sample to 1.01 g/cm^3 for the 10 mM SDS concentration. This behavior can be related to a decrease in surface tension of water caused by surfactants. Air bubbles are naturally entrapped during the mixing process, and surfactants are able to adsorb on the water-air interface of these bubbles with their hydrophobic tails towards air and their hydrophilic/polar groups towards water [28]; this stabilizes the bubbles and does not allow them to coalesce [28], which generates small nonconnected bubbles in the paste. The volume of such bubbles is significant enough to lower the density of the paste.

3.3. Reinforcing Effect of MWCNT. Since surfactants play such an important role on the density of the pastes, three-point bending tests were carried out in pairs of pastes with the same surfactant concentration, with (B) and without (P) MWCNT. The goal of this experiment was to identify the individual effects of surfactants and MWCNT on the mechanical behavior of the matrix. Previous works by the

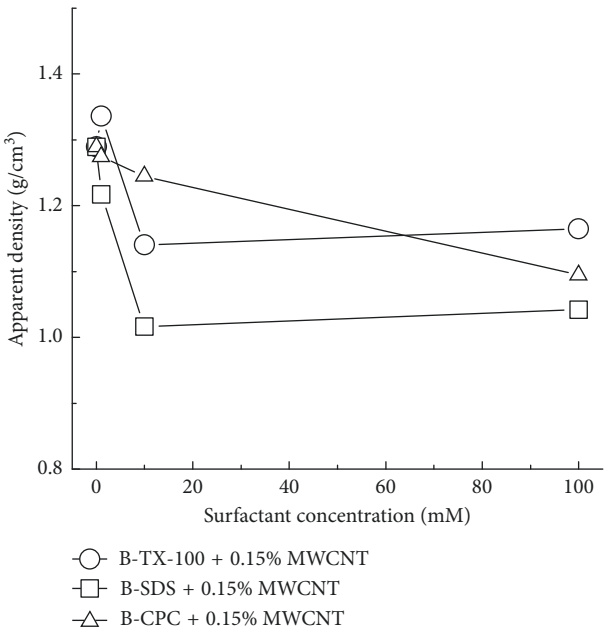

Figure 8: Apparent density of pastes with different amounts of surfactant.

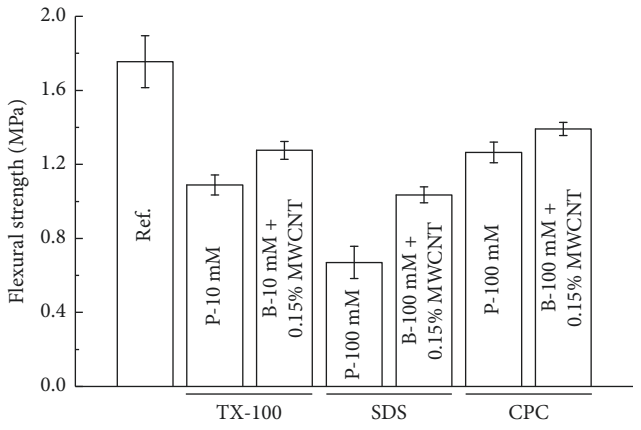

Figure 9: Flexural strength results of pastes blended with and without MWCNT and TX-100, SDS, and CPC after 7 days of curing.

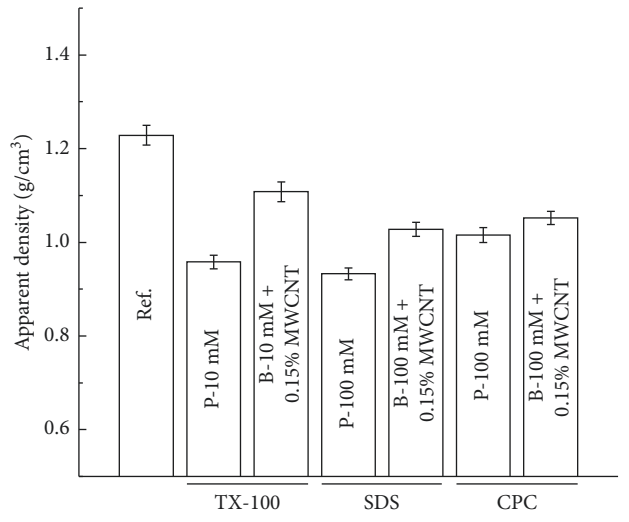

Figure 10: Apparent density of pastes tested in three-point bending.

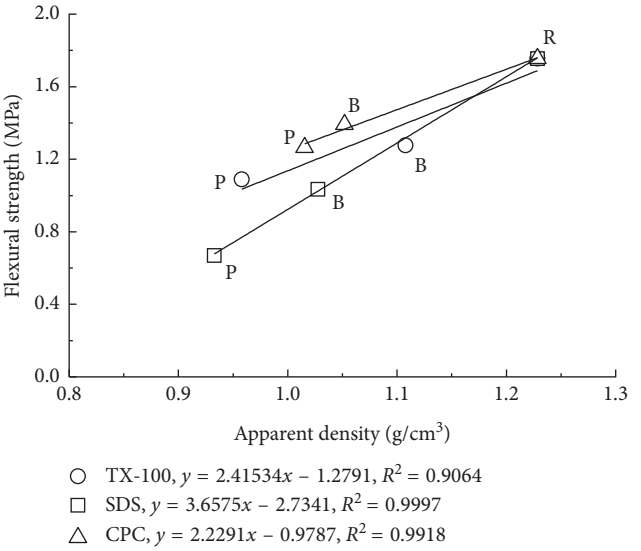

Figure 11: Apparent density versus flexural strength correlations for all pastes tested in three-point bending (P: plain paste; B: blended paste).

authors identified that for the sonication process described in the methodology, 10 mM, 100 mM, and 100 mM are the most efficient surfactant concentrations to disperse MWCNT in water for TX-100, SDS, and CPC, respectively [29]; thus, only these concentrations were used to produce samples for mechanical testing. Flexural strength results for all pastes are presented in Figure 9. It was found that flexural strength decreased for all samples when compared to the reference, regardless of the presence of MWCNT in their composition. Nevertheless, when comparing pairs of pastes with the same surfactant type and concentration, it can be seen that MWCNTs are able to improve the flexural strength of the matrix, increasing it up to 54% for the SDS case.

Apparent density was also measured for the same pastes tested in three-point bending; results are presented in Figure 10. As previously found, the presence of surfactants decreased apparent density, but pastes blended with MWCNT (B) presented an increase in these parameters when compared to their plain homologous with the same surfactant type and concentration (P). This increase can be related to a lower surfactant availability to stabilize bubbles in the matrix since a portion of the surfactant will adsorb on MWCNTs during sonication [30] and will not be available to adsorb on the water-air interface to stabilize bubbles.

A clear linear correlation between apparent density and flexural strength was found for each group of pastes with the same surfactant type and concentration, with and without MWCNT; this is presented in Figure 11. It can be seen that for each surfactant type, plain pastes always present the lowest density and the lowest flexural strength, while

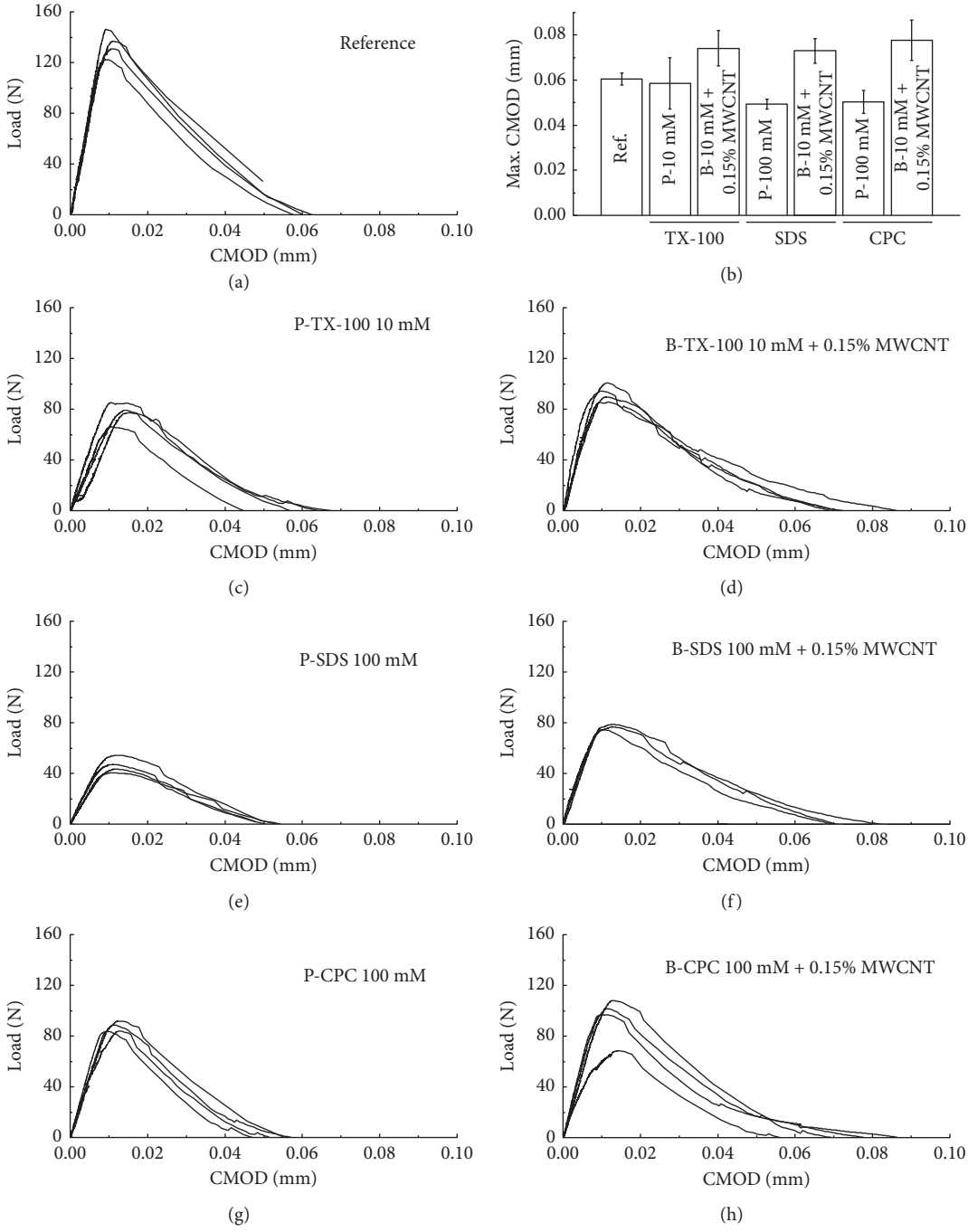

Figure 12: Load versus CMOD for all pastes tested in three-point bending.

MWCNT-blended pastes increase density and proportionally increase flexural strength. This indicates that an apparent reinforcing effect from MWCNTs can be partially related to changes in density of the paste rather than to a better load transfer between cracks due to the MWCNT.

Load versus CMOD plots for all samples tested in three-point bending are presented in Figure 12. All samples showed the same general behavior. As load was applied, there was an elastic section where deformation varied linearly with load up to the maximum load where cracking begins. This was followed immediately by a nonlinear crack growth process and a strain-softening behavior, where CMOD increases and load decreases until brakeage of the sample. No strain-hardening behavior was found in any of the samples, meaning that no multiple cracking occurred due to the presence of MWCNT in the matrix. It can be seen that the deformation at which the elastic behavior ends remains roughly constant for all the samples, regardless of the presence of surfactant or MWCNT, while the maximum deformation of the sample was increased by MWCNT, as

Table 2: Energy absorption capacity results for MWCNT-blended pastes.

Sample	D (N·mm)	$D1$ (N·mm)	$D2$ (N·mm)
B-TX-100 10 mM + CNT	0.82 ± 0.07	0.18 ± 0.02	0.64 ± 0.09
B-SDS 100 mM + CNT	0.60 ± 0.05	0.21 ± 0.01	0.39 ± 0.04
B-CPC 100 mM + CNT	0.57 ± 0.15	0.20 ± 0.07	0.37 ± 0.22

Table 3: Fracture mechanics analysis results.

Sample	E (GPa)	a_c (mm)	$a_c - a_0$ (mm)	K_{Ic}^S (Pa·m$^{1/2}$ ∗ 10^5)	CTOD$_c$ (μm)
Ref.	8.72 ± 0.62	6.03 ± 0.35	1.01 ± 0.37	3.05 ± 0.20	3.54 ± 1.01
P-TX-100 10 mM	4.44 ± 0.50	6.00 ± 0.06	0.93 ± 0.09	1.97 ± 0.09	4.37 ± 0.84
B-TX-100 10 mM + 0.15% MWCNT	6.66 ± 0.89	6.65 ± 0.47	1.54 ± 0.57	2.45 ± 0.16	4.67 ± 0.61
P-SDS 100 mM	3.27 ± 0.35	6.62 ± 0.05	1.57 ± 0.05	1.29 ± 0.13	5.14 ± 0.22
B-SDS 100 mM + 0.15% MWCNT	4.84 ± 0.09	6.76 ± 0.46	1.73 ± 0.46	1.95 ± 0.15	5.57 ± 1.26
P-CPC 100 mM	5.53 ± 0.49	6.20 ± 0.19	1.27 ± 0.10	2.35 ± 0.09	4.93 ± 0.56
B-CPC 100 mM + 0.15% MWCNT	5.76 ± 1.12	6.54 ± 0.42	1.56 ± 0.43	2.48 ± 0.23	5.72 ± 1.52

can be seen in Figure 12(b). This indicates that the enhancement in deformation induced by MWCNT is mainly in the strain-softening branch, affecting the crack opening and increasing ductility of the matrix.

Energy absorption capacity results for the pastes blended with MWCNT are presented in Table 2. It was found that up to 80% of the energy absorption capacity after peak load was contributed by the MWCNT, while the contribution from the cement matrix ($D1$) remained approximately constant at 0.20 N·mm. The contribution from the MWCNT ($D2$) varied for each type surfactant due to their different dispersion efficiencies, which depend on the polar nature and the length of the molecule [31, 32]. The reinforcing effect of MWCNT is expected to depend strongly on the dispersion degree of the individual nanotubes throughout the cement matrix [4].

Results obtained from the application of the two-parameter fracture model are presented in Table 3. It was found that E and K_{Ic}^S decreased with the presence of surfactants (P family), but a portion of this decrease was recovered with the addition of MWCNT (B family). Similarly to the flexural strength results, the decrease in mechanical performance of the P family can be related to a lower density of the matrix, and the partial recovery can be related to the reinforcing effect of MWCNT and to lower surfactant availability so stabilize bubbles.

Critical crack length (a_c) and CTOD$_c$ were increased both by surfactants and MWCNT. The increase caused by surfactants can be related to a lower E, which allows a higher deformation of the material before rupture. The increase caused by MWCNT, when comparing results from P and B families of pastes, can be associated with their reinforcing effect. It should be noticed that MWCNT increased CTOD$_c$ by less than 1 μm, which is compatible with their typical length found in the microscopy imaging.

4. General Discussion

The results found in this work showed that when using MWCNT/surfactant, aqueous dispersions surfactants decreased the density of the paste and consequently the mechanical performance of the composite. This decrease of mechanical performance was partially recovered by the presence of MWCNT, which were able to increase the strain and energy absorption capacities of the matrix, as evidenced by all the deformations measured and calculated, that is, maximum CMOD, CTOD$_c$, and K_{Ic}^S.

When comparing all the results for pastes with the same surfactant type and concentration, with and without MWCNT, the reinforcing effect of nanotubes can be clearly identified. Such effect can be divided into three different moments: (i) during the elastic regime of the deformation, where it was found that MWCNTs are capable of increasing the modulus of elasticity of the matrix due to a combination of their reinforcing effects and a lower availability of surfactant; (ii) during the crack propagation process, where it was found that MWCNTs are capable of increasing the critical opening and therefore the effective length of the crack; and (iii) during the strain-softening regime of the deformation, where it was found that MWCNTs are capable of increasing the maximum deformation and energy absorption capacity of the matrix. No strain-hardening behavior was found in any of the samples and no multiple cracking was identified, probably due to a scale incompatibility between the nanotube length and the crack width.

The reinforcing effect of MWCNTs on the mechanical behavior of cement paste was much lower than the negative effect of surfactants; this is probably due to the lack of structures that transmit tensile load at the interfaces between MWCNT and hydration products [4]. This limits the reinforcing efficiency of MWCNTs to the amount of load that the interfaces are capable of transmitting before suffering pullout, regardless of the tensile strength of the nanotubes.

5. Conclusions

It can be concluded that when using MWCNT/surfactant aqueous dispersions in a cement paste, the reinforcing effect of MWCNTs is masked by the negative effect of the

surfactants. An adequate comparison between pastes with the same type and amount of surfactant, with and without nanotubes, is necessary to identify the net reinforcing effect of nanotubes.

The increase in energy absorption capacity due to the presence of MWCNTs in the matrix could not be related to strain-hardening or multiple cracking behaviors, and this due a scale incompatibility between the nanotube length and the crack width. Nevertheless, MWCNTs are capable of increasing both stress and strain capacity of the cement matrix by controlling the crack propagation process at the tip of the crack.

Data Availability

The data used to support the findings of this study are included within the article.

Conflicts of Interest

The authors declare that they have no conflicts of interest.

References

[1] B. Wang, Y. Han, and S. Liu, "Effect of highly dispersed carbon nanotubes on the flexural toughness of cement-based composites," *Construction and Building Materials*, vol. 46, pp. 8–12, 2013.

[2] R. K. Abu Al-Rub, A. I. Ashour, and B. M. Tyson, "On the aspect ratio effect of multi-walled carbon nanotube reinforcements on the mechanical properties of cementitious nanocomposites," *Construction and Building Materials*, vol. 35, pp. 647–655, 2012.

[3] L. Y. Chan and B. Andrawes, "Finite element analysis of carbon nanotube/cement composite with degraded bond strength," *Computational Materials Science*, vol. 47, no. 4, pp. 994–1004, 2010.

[4] O. Mendoza and R. Toledo, "Nanotube–cement composites," in *Carbon Nanomaterials Sourcebook Nanoparticles, Nanocapsules, Nanofibers, Nanoporous Structures, and Nanocomposites*, K. Sattler, Ed., CRC Press, Boca Raton, FL, USA, 2016.

[5] A. Sobolkina, V. Mechtcherine, V. Khavrus et al., "Dispersion of carbon nanotubes and its influence on the mechanical properties of the cement matrix," *Cement and Concrete Composites*, vol. 34, no. 10, pp. 1104–1113, 2012.

[6] X. Ouyang, Y. Guo, and X. Qiu, "The feasibility of synthetic surfactant as an air entraining agent for the cement matrix," *Construction and Building Materials*, vol. 22, no. 8, pp. 1774–1779, 2008.

[7] B. Łaźniewska-Piekarczyk, "The influence of chemical admixtures on cement hydration and mixture properties of very high performance self-compacting concrete," *Construction and Building Materials*, vol. 49, pp. 643–662, 2013.

[8] S. Xu, J. Liu, and Q. Li, "Mechanical properties and microstructure of multi-walled carbon nanotube-reinforced cement paste," *Construction and Building Materials*, vol. 76, pp. 16–23, 2015.

[9] M. S. Konsta-Gdoutos, Z. S. Metaxa, and S. P. Shah, "Multi-scale mechanical and fracture characteristics and early-age strain capacity of high performance carbon nanotube/cement nanocomposites," *Cement and Concrete Composites*, vol. 32, no. 2, pp. 110–115, 2010.

[10] M. S. Konsta-Gdoutos, Z. S. Metaxa, and S. P. Shah, "Highly dispersed carbon nanotube reinforced cement based materials," *Cement and Concrete Research*, vol. 40, no. 7, pp. 1052–1059, 2010.

[11] F. Torabian Isfahani, W. Li, and E. Redaelli, "Dispersion of multi-walled carbon nanotubes and its effects on the properties of cement composites," *Cement and Concrete Composites*, vol. 74, pp. 154–163, 2016.

[12] S. Musso, J.-M. Tulliani, G. Ferro, and A. Tagliaferro, "Influence of carbon nanotubes structure on the mechanical behavior of cement composites," *Composites Science and Technology*, vol. 69, no. 11-12, pp. 1985–1990, 2009.

[13] Y. Hu, D. Luo, P. Li, Q. Li, and G. Sun, "Fracture toughness enhancement of cement paste with multi-walled carbon nanotubes," *Construction and Building Materials*, vol. 70, pp. 332–338, 2014.

[14] F. Collins, J. Lambert, and W. H. Duan, "The influences of admixtures on the dispersion, workability, and strength of carbon nanotube–OPC paste mixtures," *Cement and Concrete Composites*, vol. 34, no. 2, pp. 201–207, 2012.

[15] A. Hawreen, J. A. Bogas, and A. P. S. Dias, "On the mechanical and shrinkage behavior of cement mortars reinforced with carbon nanotubes," *Construction and Building Materials*, vol. 168, pp. 459–470, 2018.

[16] O. A. Mendoza Reales and R. Dias Toledo Filho, "A review on the chemical, mechanical and microstructural characterization of carbon nanotubes-cement based composites," *Construction and Building Materials*, vol. 154, pp. 697–710, 2017.

[17] M. Eftekhari, S. Mohammadi, and M. Khanmohammadi, "A hierarchical nano to macro multiscale analysis of monotonic behavior of concrete columns made of CNT-reinforced cement composite," *Construction and Building Materials*, vol. 175, pp. 134–143, 2018.

[18] M. Eftekhari, A. Karrech, M. Elchalakani, and H. Basarir, "Multi-scale modeling approach to predict the nonlinear behavior of CNT-reinforced concrete columns subjected to service loading," *Structures*, vol. 14, pp. 301–312, 2018.

[19] A. Lushnikova and A. Zaoui, "Influence of single-walled carbon nantotubes structure and density on the ductility of cement paste," *Construction and Building Materials*, vol. 172, pp. 86–97, 2018.

[20] W. Zhang, J. Ouyang, Y. Ruan et al., "Effect of mix proportion and processing method on the mechanical and electrical properties of cementitious composites with nano/fiber fillers," *Materials Research Express*, vol. 5, no. 1, pp. 1–24, 2018.

[21] M. O. Mohsen, R. Taha, A. Abu Taqa, and A. Shaat, "Optimum carbon nanotubes content for improving flexural and compressive strength of cement paste," *Construction and Building Materials*, vol. 150, pp. 395–403, 2017.

[22] X. Cui, B. Han, Q. Zheng et al., "Mechanical properties and reinforcing mechanisms of cementitious composites with different types of multiwalled carbon nanotubes," *Composites Part A: Applied Science and Manufacturing*, vol. 103, pp. 131–147, 2017.

[23] V. Papadopoulos and M. Impraimakis, "Multiscale modeling of Carbon Nanotube reinforced concrete," *Composite Structures*, vol. 182, pp. 251–260, 2017.

[24] RILEM TC 162-TDF, "Recommendations of RILEM TC 162-TDF: Test and design methods for steel fibre reinforced concrete: bending test," *Materials and Structures*, vol. 35, no. 262, pp. 579–582, 2002.

[25] Y. Jenq and S. P. Shah, "Two parameter fracture model for concrete," *Journal of Engineering Mechanics*, vol. 111, no. 10, pp. 1227–1241, 1985.

[26] A. Spagnoli, A. Carpinteri, and S. Vantadori, "Interpreting experimental fracture toughness results of quasi-brittle natural materials through multi-parameter approaches," *Frattura Ed Integrità Strutturale*, vol. 33, pp. 80–88, 2015.

[27] O. A. Mendoza-Reales, Y. P. Arias Jaramillo, J. C. Ochoa Botero, C. A. Delgado, J. H. Quintero, and R. D. Toledo, "Influence of MWCNT/surfactant dispersions on the rheology of Portland cement pastes," *Cement and Concrete Research*, vol. 107, pp. 101–109, 2018.

[28] P. Hewlett, *Lea's Chemistry of Cement and Concrete*, Elsevier Science & Technology Books, Oxford, UK, 2004.

[29] O. A. Mendoza Reales, Y. Arias, C. Delgado, J. Ochoa, J. Quintero, and R. D. Toledo, "Surfactants as dispersants for carbon nanotubes in water: hydration of cement," in *Proceedings of the 10th ACI/RILEM International Conference on Cementitious Materials and Alternative Binders for Sustainable Concrete*, pp. 1–15, Montreal, QC, Canada, October 2017.

[30] L. Jiang, L. Gao, and J. Sun, "Production of aqueous colloidal dispersions of carbon nanotubes," *Journal of Colloid and Interface Science*, vol. 260, no. 1, pp. 89–94, 2003.

[31] Y. Tan and D. E. Resasco, "Dispersion of single-walled carbon nanotubes of narrow diameter distribution," *Journal of Physical Chemistry B*, vol. 109, no. 30, pp. 14454–14460, 2005.

[32] R. Rastogi, R. Kaushal, S. K. Tripathi, A. L. Sharma, I. Kaur, and L .M. Bharadwaj, "Comparative study of carbon nanotube dispersion using surfactants," *Journal of Colloid and Interface Science*, vol. 328, no. 2, pp. 421–428, 2008.

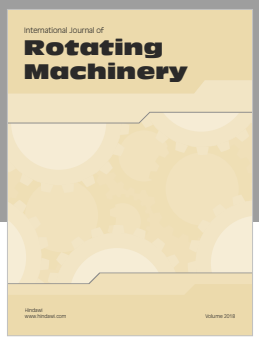

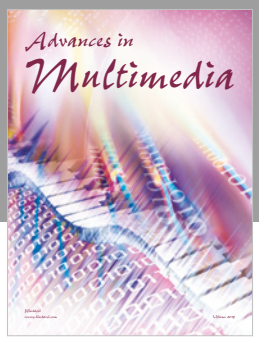

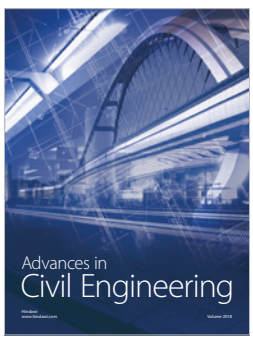

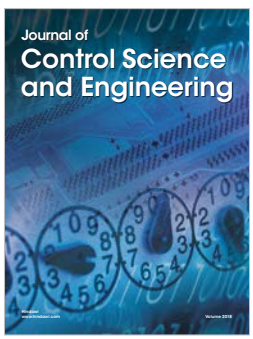

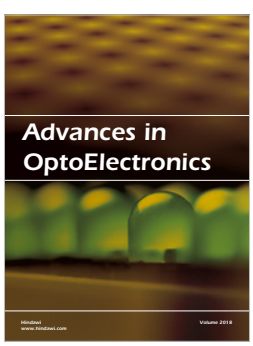

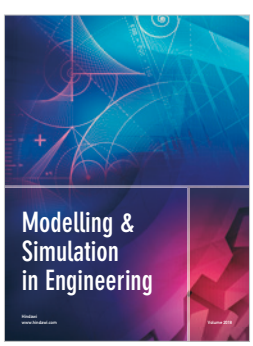

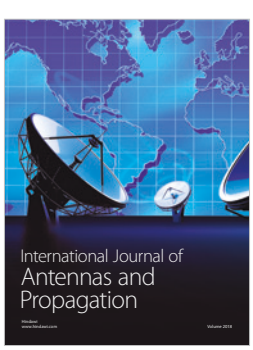

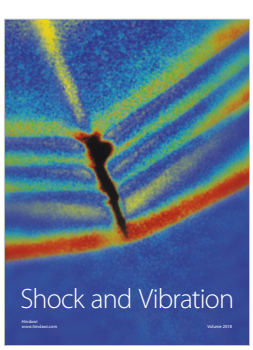

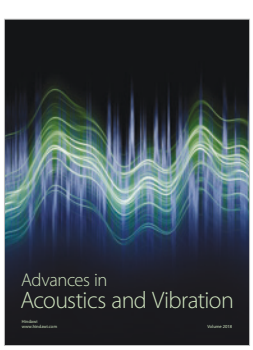

Hindawi

Submit your manuscripts at
www.hindawi.com